



Bioresorbable zinc stent with ultra-thin center struts attenuates stent jail in porcine femoral artery bifurcations

Christoph Hehrlein, Björn Schorch, Jörg Haberstroh, Christoph Bode, Lilli Mey, Hans Schwarzbach, Ralf Kinscherf, Stephan Meckel, Stefanie Schiestel, Adalbert Kovacs, Harald Fischer & Ernst Nennig

To cite this article: Christoph Hehrlein, Björn Schorch, Jörg Haberstroh, Christoph Bode, Lilli Mey, Hans Schwarzbach, Ralf Kinscherf, Stephan Meckel, Stefanie Schiestel, Adalbert Kovacs, Harald Fischer & Ernst Nennig (2020): Bioresorbable zinc stent with ultra-thin center struts attenuates stent jail in porcine femoral artery bifurcations, *Minimally Invasive Therapy & Allied Technologies*, DOI: [10.1080/13645706.2020.1770797](https://doi.org/10.1080/13645706.2020.1770797)

To link to this article: <https://doi.org/10.1080/13645706.2020.1770797>



© 2020 The Author(s). Published by Informa UK Limited, trading as Taylor & Francis Group



Published online: 13 Jun 2020.



Submit your article to this journal [↗](#)



Article views: 497



View related articles [↗](#)





View Crossmark data [↗](#)



Citing articles: 2 View citing articles [↗](#)

Bioresorbable zinc stent with ultra-thin center struts attenuates stent jail in porcine femoral artery bifurcations

Christoph Hehrlein^a, Björn Schorch^a , Jörg Haberstroh^b , Christoph Bode^a, Lilli Mey^c, Hans Schwarzbach^c, Ralf Kinscherf^c, Stephan Meckel^d, Stefanie Schiestel^e, Adalbert Kovacs^e, Harald Fischer^f and Ernst Nennig^f

^aDepartment of Cardiology and Angiology I, Heart Center – University of Freiburg, Faculty of Medicine, University of Freiburg, Freiburg, Germany; ^bDivision of Experimental Surgery, Center for Experimental Models and Transgenic Services, Medical Center – University of Freiburg, Faculty of Medicine, University of Freiburg, Freiburg, Germany; ^cInstitute for Anatomy and Cell Biology, Dept. of Medical Cell Biology, Philipps-University Marburg, Marburg, Germany; ^dDepartment of Neuroradiology, Medical Center – University of Freiburg, Faculty of Medicine, University of Freiburg, Germany; ^eLimedion GmbH, Mannheim, Germany; ^fOptimed GmbH, Ettlingen, Germany

ABSTRACT

Introduction: An ultra-thin, fracture-resistant and bioresorbable stent may be advantageous for provisional stenting in vessel bifurcations, if catheter passage and side-branch post-dilatation is facilitated to prevent a ‘stent jail’ by struts obstructing the orifice of a major side branch.

Material and methods: We studied a highly radiopaque, slowly bioresorbable zinc alloy stent characterized by a novel design of a radiopaque-marked region of ultra-thin struts in the center of the stent. The stent is characterized by an extended range flexibility and high fracture resistance. Zn-stents and Zn-drug eluting stents (DES) were implanted opposite to rigid Nitinol stents into both femoral artery bifurcations of 21 juvenile pigs, followed for one and three months and studied by angiography and histomorphometry.

Results and conclusion: Bare Zn-stents with thinner stent struts showed less neointimal hyperplasia compared to Zn-stents with thicker struts. Neointimal formation was further reduced by 12% in Zn-alloy DES. Both, bare Zn-stents and Zn-DES, can be precisely positioned into the femoral artery bifurcation, allowing easy balloon catheter passage through the very thin strut mesh. Side branch orifices remained open after Zn-stent deployment without stent jailing. No stent fractures or particles emboli occurred after the deployment. A Zn-stent with ultra-thin center struts may be useful for provisional stenting in vessel bifurcations.

ARTICLE HISTORY

Received 20 December 2019
Accepted 21 April 2020



KEYWORDS

Drug eluting stent; fracture-resistant; provisional stenting; ultra-thin; zinc

Introduction

It has been previously shown that the biocompatibility of vascular stents depends on the mesh thickness of each individual stent strut [1]. A thick stent strut causes more neointimal hyperplasia, i.e., vessel lumen narrowing than a thin strut [1]. Stent fractures and collapse causing lumen occlusions by vessel thrombosis or stenosis can occur if the struts are too brittle, too thick or are made from polymers with low mechanical stability such as poly-L-lactic acid (PLLA) [2–4]. Vessel segments containing large side branches (bifurcations) and small vessels are contraindicated for the use of otherwise FDA-approved bioresorbable stents made from PLLA [5]. Stent struts can cause

side branch occlusion after stent placement in the main vessel [6]. A so called ‘stent-jail’ severely obstructing the orifice of the side branch after provisional stenting of the main vessel branch is a serious problem of percutaneous interventions applying stents in arterial bifurcations [6]. In femoral artery bifurcations, therefore, open vascular surgery is still the treatment of choice for arteriosclerotic lesions and stent interventions are rarely performed [7,8]. The stent-jail is a well characterized entity of lumen narrowing or stenosis of the side branch orifice by stent struts complicating a catheter passage through the stent mesh in order to repair the vascular damage and prevent causing side branch occlusions [6].

CONTACT Christoph Hehrlein  christoph.hehrlein@universitaets-herzzentrum.de  Department of Cardiology and Angiology I, Heart Center – University of Freiburg, Faculty of Medicine, University of Freiburg, Hugstetter Str. 55, Freiburg, D-79106, Germany
This article has been republished with minor changes. These changes do not impact the academic content of the article.

© 2020 The Author(s). Published by Informa UK Limited, trading as Taylor & Francis Group

This is an Open Access article distributed under the terms of the Creative Commons Attribution-NonCommercial-NoDerivatives License (<http://creativecommons.org/licenses/by-nc-nd/4.0/>), which permits non-commercial re-use, distribution, and reproduction in any medium, provided the original work is properly cited, and is not altered, transformed, or built upon in any way.

We studied a novel bioresorbable zinc (Zn) alloy stent characterised by a high elongation-to-fracture rate, flexibility and mechanical stability designed with ultra-thin center struts to ease catheter access to the major side branch and to prevent ‘stent-jail’ of the major side branch. Ultra-thin center struts placed at the orifice of the large side branch may allow easier catheter passage, may facilitate post-dilatation and improving re-opening of side branch orifices after provisional stenting of the main branch. Bioresorbable Zn stent struts can degrade slowly and generally disappear within a period of 12–24 months after stent implantation [9], which preserves stent integrity for proper vessel scaffolding. The primary study hypothesis was to investigate the outcome of single ‘provisional’ stenting of the main branch of the femoral artery bifurcation applying a novel fracture-resistant bioresorbable stent featuring reduced sizes of its center struts with the aim to keep the major side branch orifice of the bifurcation open. A porcine common femoral artery bifurcation model was used to test this hypothesis.

Material and methods

Stent manufacture

Zinc alloy was prepared and a stent was manufactured as described previously [9]. Zn-alloy stents (length 20 mm) for femoral artery use expandable to an outer diameter of 6 mm were produced as open-cell stents at a length of 20 mm. In the first stent design (D1), a strut thickness of 229 μm of rectangular struts was produced which transformed into a strut thickness reduced by 25% in the stent center (ultra-thin design, 172 μm). The ultra-thin strut area in the stent center was designated with two radiopaque platinum markers (Figure 1). The second design (D2) was characterized by a strut thickness of

167 μm and a further 25% reduction of the strut thickness in the stent center (ultra-thin design, 125 μm). The third design (D3) was characterized by rectangular 176 μm thick struts coated with a PLLA layer eluting sirolimus at a dose of 2.1 $\mu\text{g}/\text{mm}^2$ stent surface area. The stent delivery balloon system was equipped with a radiopaque marker at its distal end in order to precisely steer the ultra-thin strut region facing the sidebranch orifice (Figure 1). As control stents, commercial available self-expanding Nitinol stents (length 20 mm, expanded diameter 6 mm, 215 μm strut thickness) were used and implanted in the contralateral porcine femoral bifurcation according to the manufacturer instructions.

Bench tests

A silicone tube model (bifurcating polymer tubing of 6 mm diameter) mimicking the femoral artery bifurcation was developed (Figure 2(A)). A balloon expandable Zn alloy stent with ultra-thin center struts was implanted into one branch of the tubing of the bifurcation of the two branches such that the ultra-thin struts of the stent center are facing the orifice of one branch of the silicone tubing. After stent deployment, another balloon catheter was passed through the ultra-thin strut mesh into the side branch for post-dilatation of the ultra-thin zinc alloy struts (Figure 2(B)). A post-dilatation balloon catheter was removed after optimization of the access to the side branch after a balloon dilatation leaving a wide open side branch orifice behind (Figure 2(C)).

Animal model

Animal experiments were performed according to the standard of care outlined in the ARRIVE guidelines of animal research [10] and were approved by the federal animal care ethics committee (#35-9.185.81).

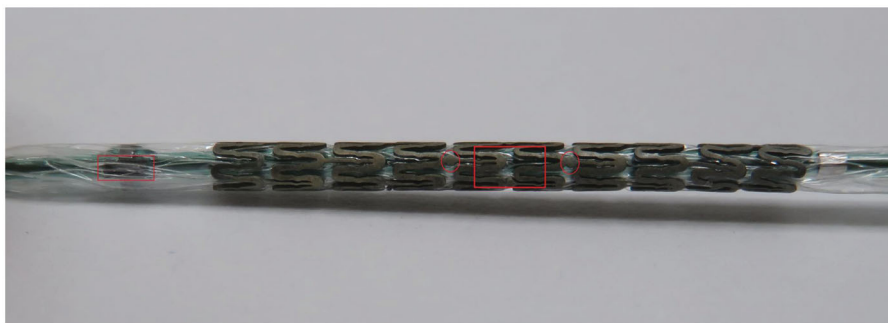


Figure 1. A zinc-stent crimped onto a stent delivery balloon. Circles indicate the radiopaque positioning markers of the ultra-thin strut region. The rectangular bar indicates the area of ultra-thin strut size. The flat bar indicates the radiopaque positioning marker of the distal balloon tip

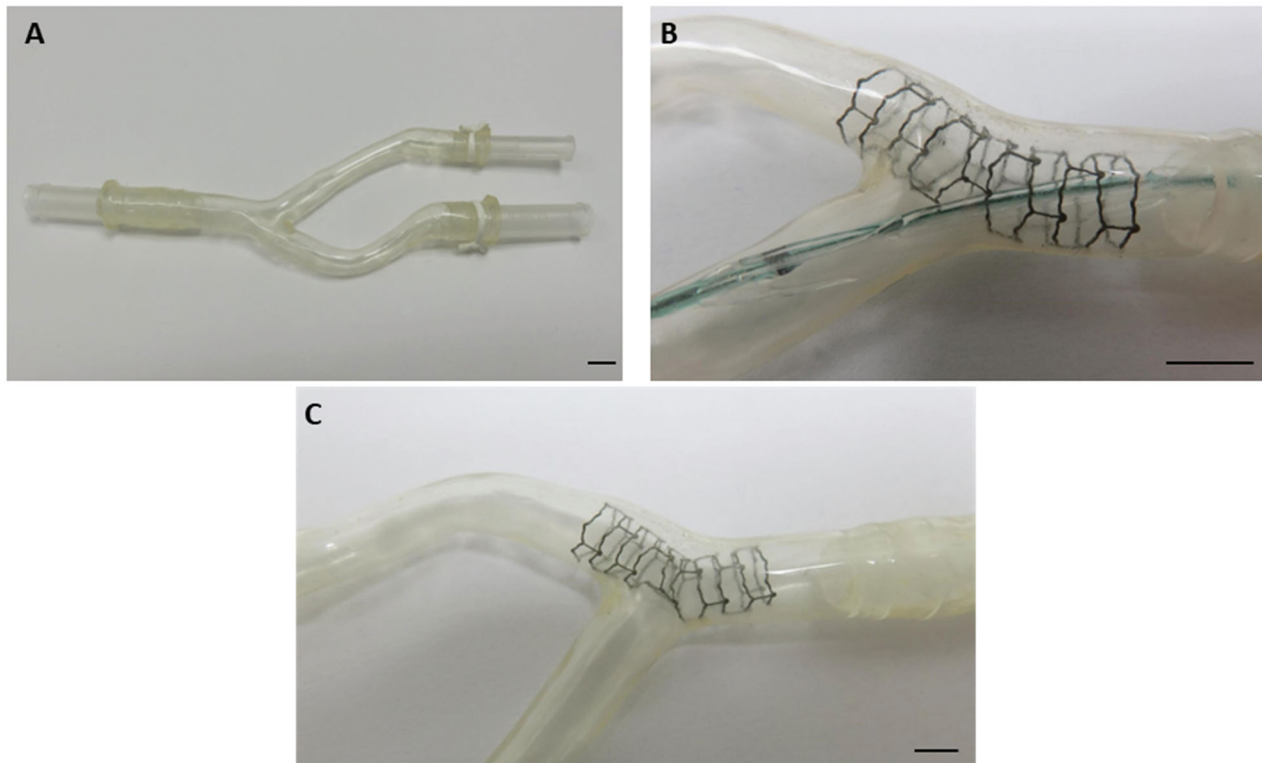


Figure 2. 'Ex vivo' silicon tube bifurcation model (A). (B) shows a zinc-stent after implantation into one tube with the stent center facing the orifice of the other tube. (C) indicates the result after balloon dilatation through the mesh of the ultra-thin center struts to further open the sidebranch orifice and prevent side branch stent jail in the model. The marker represents 5 mm.

Experiments were performed on juvenile domestic swine (36 ± 4 kg bodyweight) of equal sex distribution. All animals received ASS and clopidogrel one day prior to stent implantation and until termination. Pre-interventional swine were fasted 12 h and medicated with 0.5 mg kg^{-1} midazolam and 20 mg kg^{-1} ketamine hydrochloride i.m. General anaesthesia was induced with i.v. administration of $2\text{--}4 \text{ mg kg}^{-1}$ propofol and maintained by inhalation of 1.5–2.5% isoflurane and injection of $4 \mu\text{g kg}^{-1} \text{ h}^{-1}$ fentanyl citrate. Muscle relaxation was obtained by administration $0.2 \text{ mg kg}^{-1} \text{ h}^{-1}$ vecuronium. After tracheal intubation, the lungs were ventilated in the volume-controlled mode at a PEEP of 8 cm H_2O . Inspired oxygen fraction (FIO_2) was maintained at a rate of 0.3. Respiratory rate and tidal volume were adjusted to keep end-expiratory CO_2 physiological. Ringer's solution was infused at $10 \text{ ml kg}^{-1} \text{ h}^{-1}$. The carotid artery was accessed by surgical cut-down. Before catheterizing the arterial system, heparin (10,000 IU) was administered to maintain activated clotting time >250 s. A total 21 of swine received endovascular provisional stenting of the main branch of the common femoral artery bifurcation. A standard rigid, self-expanding vascular Nitinol stent (final diameter 6 mm) was implanted as a control into the contralateral femoral artery bifurcation. Follow-up angiography and histopathology were

performed after one month ($n = 14$) and three months ($n = 7$).

Histomorphometry

Stented arterial samples were dehydrated in acetone and embedded in hydroxyethyl-methacrylate (Technovit 8100, Kulzer, Hanau, Germany). After polymerization, the stents were cut using a rotary diamond saw (Leica SP 1600, Leica Biosystems, Nussloch, Germany) into $300 \mu\text{m}$ -thick cross-sections and ground and polished into $40\text{--}60 \mu\text{m}$ -thick sections using a disc sander (Exakt 400CS, EXAKT Advanced Technologies, Norderstedt, Germany). Side branch opening diameter and percentage of strut stent jailing was measured independently by two histopathologists with the use of ImageJ software. An idealized circular line was used to follow the cross-sectional course of stent struts and record struts located in the side branch orifice. The free orifice was determined as follows: free orifice (in mm) = side branch orifice (mm) – sum of struts (mm). Side branch obstruction caused by struts was calculated as follows: stent jailing (in %) = $100 \times \text{sum of all strut lengths (in mm)}/\text{side branch orifice (in mm)}$. Arterial cross-sections were analysed regarding neointimal formation, including measurement of neointimal area (mm^2), neointimal thickness

(μm) and external elastic lamina area (mm^2) by the method of Murphy and Schwartz [11].

Statistics

Statistical analysis was performed with SigmaPlot 14.0 and graphic data representations were generated by Microsoft Excel. Significance for the comparison of multiple groups were analyzed by a multivariate ANOVA with a following pairwise comparison using Kruskal Wallis One Way Variance Analysis. Significance levels were illustrated as follows: * $p < .05$; ** $p < .01$; *** $p < .005$.

Results

Bench tests in a silicone bifurcation model

The bench test of stent deployment in a silicon tube bifurcation model showed simple positioning and deployment of the stent with its ultrathin-strut region in the stent center facing the orifice of the side branch. Stent expansion of the ultra-thin center region did not cause any stent strut breakage or cracks and fissure in the stent surface. The tests were specifically designed to investigate mechanical stability after stent deployment.

Animal welfare at follow-up

All studied pigs were without signs of any physical disability throughout the study periods of four weeks and 12 weeks. The pigs were able to walk immediately after the procedure of femoral bifurcation stenting and waking up from anesthesia. No clinical signs of stent occlusion by thrombosis or signs of stent particle embolization into the legs of the pigs were noted during the follow-up of one and three months.

Angiographic results of stenting the femoral artery bifurcation of pigs

Angiographic signs of a stent jail of the side branch orifice were noted in the follow-up of 2 out of 21 bifurcations stented with a self-expanding Nitinol stent (control) and in none of the 21 bifurcations stented with Zn alloy stents (bare or drug coated) designed with ultrathin center struts (Figure 3(A,B)).

Histomorphometry of stented femoral arteries

Zn-stents with a smaller strut thickness showed less cross-sectional neointimal formation reduced by 32% compared

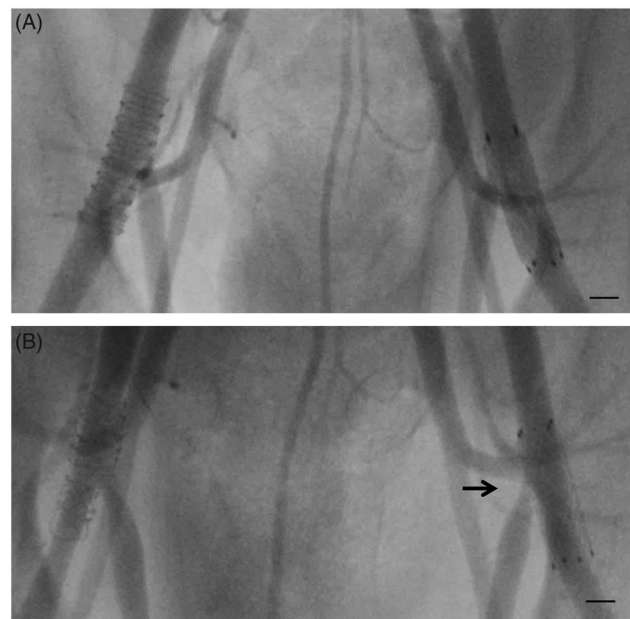


Figure 3. Post-interventional angiography displaying the acute implantation result of a Nitinol stent (left femoral artery, right side of X-ray image) and zinc stent featuring ultrathin center struts (right femoral artery, left side of X-ray image) (A) and at the 12-week follow up investigation (B). The arrow indicates the side branch jailing of the Nitinol stent (B) after 12 weeks. The marker represents 5 mm.

with stents of thicker strut thickness (9.9 ± 0.5 vs. $14.5 \pm 1.1 \text{ mm}^2$, $p < .05$), which was further reduced by 12% applying an anti-proliferative drug coating (8.7 ± 1.2 vs. $9.9 \pm 0.5 \text{ mm}^2$, $p < .05$). Self-expanding Nitinol control stents induced significantly more vessel expansion in juvenile pig femoral arteries than balloon-expandable Zn alloy stents and created comparatively small amounts of cross-sectional neointimal formation (Table 1).

Struts of Zn alloy were mainly located in the periphery of the side branch ostium and were at this region covered with endothelium (Figure 4(A,C)), whereas Nitinol struts pervaded and covered the side branch orifice, caused stent jailing and were not endothelialized (Figure 4(B,D)). In the four-week follow-up study, Nitinol stents showed a stent jail rate of $21\% \pm 7.3$ in comparison to Zn alloy with $17.3\% \pm 3.2$ (D2, $n = 6$) and $14.2\% \pm 4.8$ (D3, $n = 4$). We did not detect significant differences in side branch stent jailing between the study groups at the four-week follow-up period. However, after 12 weeks Nitinol stents ($n = 7$) showed a significant higher stent jail rate ($38.9\% \pm 4.1$) than Zn alloy ($4.8\% \pm 4.8$, D2, $n = 4$), (Table 2).

Discussion

Although peripheral arterial diseases (PAD) are developing into an expanding field for endovascular

Table 1. Cross-sectional neointimal areas assessed by histomorphometry of bare Zn stents designed with thick struts (D1), with thin-struts (D2) and thin struts coated with an anti-proliferative drug coating (D3) and Nitinol stents.

	D1	D2	D3	Nitinol
Neointimal area (mm ²)	14.41 ± 1.10	9.88 ± 0.48*	8.68 ± 1.20*	6.13 ± 0.56*
Neointimal thickness (μm)	1207.3 ± 70.0	854.8 ± 70.9*	664.6 ± 41.3*	403.5 ± 19.0*
Vessel area (EEL) (mm ²)	28.48 ± 1.25	24.47 ± 0.32*	33.47 ± 4.60*	36.6 ± 0.82*

All investigated zinc alloy stent groups featured the ultra-thin center struts design and were implanted with a stent delivery balloon directing the ultra-thin strut area towards the side branch orifice. Nitinol control stents with standard strut thicknesses were implanted into the contralateral femoral artery bifurcation. * indicates a significant difference compared to the first-generation zinc alloy stents ($p < .05$).

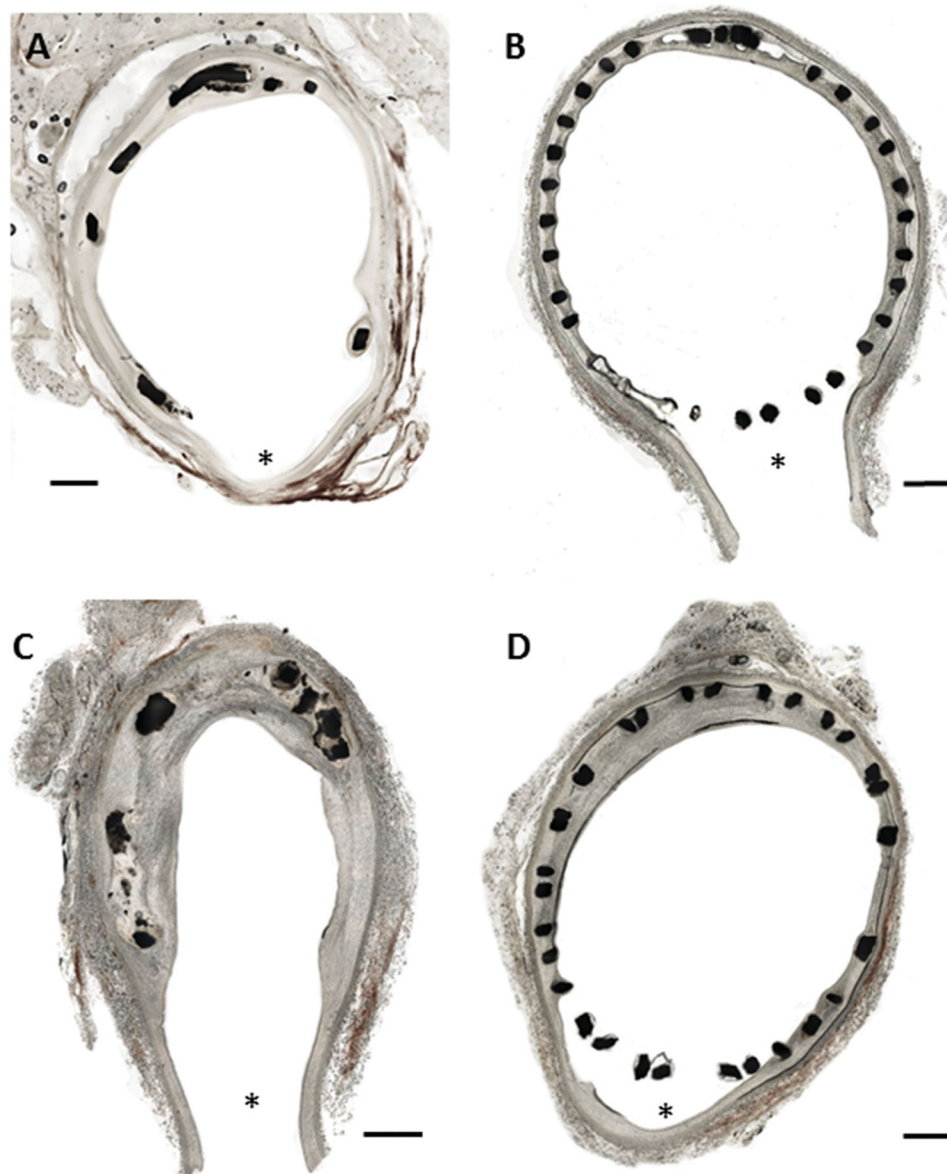


Figure 4. Histopathological cross-sections of pig arteries four weeks after implantation of a drug eluting coated zinc alloy of a thicker strut design (176 μm) D3 (A) and a standard Nitinol control stent (B) in the femoral artery bifurcation at the orifice of the sidebranch (indicated by *). C shows a cross section 12 weeks after implantation of a bare zinc alloy stent in comparison to a Nitinol stent after the same time (D). The scale bar represents 1 mm. The struts of the control stent cover the orifice of the side-branch indicating a so called 'stent jail'.

interventions using bioresorbable stents [12], bifurcation stenting in PAD is rare. More clinical experience with bifurcation stenting exists in coronary artery

lesions, e.g., in vessels of diameters of 2–4 mm [13–17]. Stenting of the main arterial branch and balloon dilatation only of the side branch (so-called

Table 2. Histomorphometric measurements of sidebranch opening after provisional stenting.

	D2 (4 weeks)	D3 (4 weeks)	Nitinol (4 weeks)	D2 (12 weeks)	Nitinol (12 weeks)
Free side branch orifice (mm)	2.7 ± 0.3	2.6 ± 0.2	2.6 ± 0.2	1.8 ± 0.3***	2.4 ± 0.2
Side branch stent jailing (%)	17.3 ± 3.2	14.2 ± 4.8	21.0 ± 7.3	4.8 ± 4.8***	38.9 ± 4.1

Orifice jailing and free orifice of the side branch was measured on at least 4 different pig arteries. *** indicates $p < .001$ vs. Nitinol 12 weeks.

‘provisional stenting’) is an accepted method of catheter-based endovascular treatment of bifurcation lesions [16]. However, ‘jailing’ a major side branch with a stent by occluding the side branch with its stent struts can jeopardize vessel patency by side branch occlusion and subsequent infarction [17]. In diabetic patients, in eccentric lesions, and small vessels, PLLA (Absorb) or Mg (Magmaris) stents should be used with cautions [18–21]. Moreover, time consuming lesion preparation with multiple balloon dilatations and extensive post-interventional endovascular imaging for proper stent apposition are considered a disadvantage for the clinical use of bioresorbable stents of low mechanical stability such PLLA or Mg-stents [22].

In addition, bioresorbable stents made from PLLA (Absorb) or Magnesium (Magmaris) are contraindicated for use in bifurcation lesions, because their clinical performance and outcomes in this region was not satisfying [5,23].

Multiple dilatations of a stent using a balloon to optimize stent results (post-dilatation) can cause stent fractures. Even in conventional, non-degradable stents made from cobalt chromium, stent fracture rates occur in 3–7% of all cases and lead to serious side effects [24,25]. In some bioresorbable stents such as Mg-stents, stent fracture and collapse occur particularly after post-dilatation [26].

The hypothesis of this work was to test whether a novel bioresorbable metallic stent with ultra-thin center struts (25% reduction of strut thickness vs. proximal and distal stent ends) helps to prevent a stent jail of the major side branch after implantation in a bifurcation lesion.

The specific Zn-alloy used in this study has a unique material advantage of high flexibility and fracture resistance versus pure zinc and non-degradable stent materials such as cobalt chromium or Nitinol stents. Especially, if balloon dilatation through the stent strut mesh is necessary to treat vessel side branches ultra-thin, fracture-resistant struts may be advantageous. Furthermore, non-degradable Nitinol is a memory-shaped material, which tends to resume its initial shape after being post-dilated with a balloon. We previously described the high fracture resistance of the alloy material even at high mechanical forces which makes it a better candidate than pure zinc for

designing reduced strut thicknesses to ease catheter access to side branch orifices and to prevent stent jail.

Zn stents have been recently discovered as potential candidates for the production of bioresorbable stents because of their favorable degradation pattern [27]. We have previously demonstrated that zinc-alloyed with minimal amounts of silver (Ag) contributes to its high mechanical stability and unique fracture resistance and improves the mechanical characteristics of pure zinc material [9]. Zinc stents are characterized by a fairly slow degradation pattern and equal biocompatibility compared with PLLA or Magnesium stent materials [9]. The Zn-stent bioresorption occurs much slower than that of clinically used Mg-alloy stents and is slightly faster than that of PLLA stent materials ranging from 12 to 24 months [9,28]. After a period of 6–12 months, Zn-stents are resorbed by 20–30% within the vessel wall but are already completely endothelialized after one month [9,28].

In this study, we demonstrate that Zn alloy stents with flexible, ultra-thin center struts can be expanded with a standard stent delivery balloon without inducing stent strut fractures. Moreover, ultrathin stent struts can be post-dilated with ease optimizing endovascular treatment of the side branch orifice. The observed favorable results are due to the fact that the tested Zn alloy stent material is characterized by a high elongation-to-fracture rate which prevented stent surface cracks and fissures or strut breakage in this study. No embolization of any stent particles was noted. We corroborated earlier clinical data that a stent design with thicker stent struts leads to more neointimal formation, and that a thin stent strut design should be preferred if stent performance and mechanical stability are unaltered. In addition, we demonstrate advantages for a Zn-alloy stent coated with a sirolimus eluting PLLA layer (Zn-DES) by reducing post-interventional neointimal formation in the vessel.

Declaration of interest

C.H., A.K., S.S., H.F., and E.N. filed patent applications; Limedion GmbH and optimed GmbH are manufacturers of stent materials, stents and catheters.

Funding

The authors thank the BMBF Research Foundation, Germany, for financial support [13GW0035B] of this study. Any opinions, findings, and conclusions or recommendations expressed in this material are those of the authors and do not necessarily reflect the views of the BMBF.

ORCID

Björn Schorch  <http://orcid.org/0000-0001-8311-0210>
 Jörg Haberstroh  <http://orcid.org/0000-0001-6483-3691>

References

- [1] Briguori C, Sarais C, Pagnotta P, et al. In-stent restenosis in small coronary arteries: impact of strut thickness. *J Am Coll of Cardiol.* 2002;40:403–409.
- [2] Elwany M, Di Palma G, Cortese B. Fracture with the newer bioresorbable vascular scaffolds. *Catheter Cardiovasc Interv.* 2017;90:582–583.
- [3] Foin N, Lee R, Bourantas C, et al. Bioresorbable vascular scaffold radial expansion and conformation compared to a metallic platform: insights from in vitro expansion in a coronary artery lesion model. *EuroIntervention.* 2016;12:834–844.
- [4] Diletti R, Tchetche D, Barbato E, et al. Bioresorbable scaffolds for treatment of coronary bifurcation lesions: critical appraisal and future perspectives. *Catheter Cardiovasc Interv.* 2016;88:397–406.
- [5] Steinvil A, Rogers T, Torguson R, et al. Overview of the 2016 U.S. JACC Cardiovasc Interv. 2016;9:1757–1764.
- [6] Yamawaki M, Hirano K, Nakano M, et al. Deployment of self-expandable stents for complex proximal superficial femoral artery lesions involving the femoral bifurcation with or without jailed deep femoral artery. *Cathet Cardiovasc Intervent.* 2013;81:1031–1041.
- [7] Siracuse JJ, Van Orden K, Kalish JA, et al.; Vascular Quality Initiative. Endovascular treatment of the common femoral artery in the Vascular Quality Initiative. *J Vasc Surg.* 2017;65:1039–1046.
- [8] Ansel G. Keep out of jail: the reason to limit stent usage for the common femoral artery bifurcation. *Catheter Cardiovasc Interv.* 2013;81:1042.
- [9] Hehrlein C, Schorch B, Kress N, et al. Zn-alloy provides a novel platform for mechanically stable bioresorbable vascular stents. *Plos One.* 2019;14:e0209111.
- [10] Kilkenny C, Browne WJ, Cuthill IC, et al. Improving bioscience research reporting: the ARRIVE guidelines for reporting animal research. *PLoS Biol.* 2010;8:e1000412.
- [11] Murphy JG, Schwartz RS, Edwards WD, et al. Percutaneous polymeric stents in porcine coronary arteries. Initial experience with polyethylene terephthalate stents. *Circulation.* 1992;86:1596–1604.
- [12] Werner M, Micari A, Cioppa A, et al. Evaluation of the biodegradable peripheral Igaki-Tamai stent in the treatment of de novo lesions in the superficial femoral artery: the GAIA study. *JACC Cardiovasc Interv.* 2014;7:305–312.
- [13] Kwon O, Ahn JM, Kang DY, et al. Early experience and favorable clinical outcomes of everolimus-eluting bioresorbable scaffolds for coronary artery disease in Korea. *Korean J Intern Med.* 2018;33:922–932.
- [14] Adjedj J, Picard F, Mogi S, et al. In vitro flow and optical coherence tomography comparison of two bailout techniques after failed provisional stenting for bifurcation percutaneous coronary interventions. *Catheter Cardiovasc Interv.* 2019;93:E8–E16.
- [15] Chen X, Zhang D, Yin D, et al. Can “true bifurcation lesion” actually be regarded as an independent risk factor of acute side branch occlusion after main vessel stenting?: a retrospective analysis of 1,200 consecutive bifurcation lesions in a single center. *Cathet Cardiovasc Intervent.* 2016;87:554–563.
- [16] Généreux P, Kumsars I, Lesiak M, et al. A randomized trial of a dedicated bifurcation stent versus provisional stenting in the treatment of coronary bifurcation lesions. *J Am Coll Cardiol.* 2015;65:533–543.
- [17] Naganuma T, Colombo A, Lesiak M, et al. Bioresorbable vascular scaffold use for coronary bifurcation lesions: a substudy from GHOST EU registry. *Catheter Cardiovasc Interv.* 2017;89:47–56.
- [18] Serruys PW, Chevalier B, Sotomi Y, et al. Comparison of an everolimus-eluting bioresorbable scaffold with an everolimus-eluting metallic stent for the treatment of coronary artery stenosis (ABSORB II): a 3 year, randomised, controlled, single-blind, multicentre clinical trial. *Lancet.* 2016;388:2479–2491.
- [19] Suwannasom P, Sotomi Y, Asano T, et al. Change in lumen eccentricity and asymmetry after treatment with Absorb bioresorbable vascular scaffolds in the ABSORB cohort B trial: a five-year serial optical coherence tomography imaging study. *EuroIntervention.* 2017;12:e2244–e2252.
- [20] Haude M, Ince H, Abizaid A, et al. Safety and performance of the second-generation drug-eluting absorbable metal scaffold in patients with de-novo coronary artery lesions (BIOSOLVE-II): 6 month results of a prospective, multicentre, non-randomised, first-in-man trial. *Lancet.* 2016;387:31–39.
- [21] Capranzano P, Capodanno D, Brugaletta S, et al. Clinical outcomes of patients with diabetes mellitus treated with Absorb bioresorbable vascular scaffolds: a subanalysis of the European Multicentre GHOST-EU Registry. *Catheter Cardiovasc Interv.* 2018;91:444–453.
- [22] Giblett JP, Brown AJ, Hoole SP, et al. Early disarticulation of a bioresorbable vascular scaffold: an underreported consequence of repeat imaging. *Cardiovasc Interv Ther.* 2018;33:175–177.
- [23] Campos CM, Lemos PA. Bioresorbable vascular scaffolds: novel devices, novel interpretations, and novel interventions strategies. *Catheter Cardiovasc Interv.* 2014;84:46–47.
- [24] Conway C. Coronary stent fracture: clinical evidence vs. the testing paradigm. *Cardiovasc Eng Technol.* 2018;9:752–760.

- [25] Kapnisis K, Constantinides G, Georgiou H, et al. Multi-scale mechanical investigation of stainless steel and cobalt-chromium stents. *J Mech Behav Biomed Mater.* 2014;40:240–251.
- [26] Marynissen T, McCutcheon K, Bennett J. Early collapse causing stenosis in a resorbable magnesium scaffold. *Catheter Cardiovasc Interv.* 2018;92: 310–312.
- [27] Bowen PK, Shearier ER, Zhao S, et al. Biodegradable Metals for Cardiovascular Stents: from Clinical Concerns to Recent Zn-Alloys. *Adv Healthc Mater.* 2016;5:1121–1140.
- [28] Yang H, Wang C, Liu C, et al. Evolution of the degradation mechanism of pure zinc stent in the one-year study of rabbit abdominal aorta model. *Biomaterials.* 2017;145:92–105.